

Hydrodynamic study of energy harvesting breakwater with parabolic openings

Chongwei ZHANG **, Dezhi NING †*, and Bin TENG ‡*

*State Key Laboratory of Coastal and Offshore Engineering, Dalian University of Technology, Dalian 116023, China

Commercialization of wave energy converters (WECs) is still restricted by the challenge of energy conversion efficiency at present. To help improve the efficiency, a proportion of researches has put great effort into optimising geometry [1] or spatial layout [2] of WEC devices, many of which have given good results. Even so, current literature review indicates that the efficiency improvement still has a 'ceiling limit', and even 10% increase of the efficiency is hard to achieve solely through a geometry optimization[3]. From the coastal engineering background, some recent studies show that an integration of WECs into the breakwater can help increase the conversion efficiency due to a wave amplitude magnification after wave reflection in front of the breakwater[4]. Moreover, the economic burden can be greatly reduced through the cost sharing of WECs and breakwaters during construction.

This study will investigate a further improvement of the WEC-breakwater integration. Enlightened by a parabolic reflector that can reflect sound towards a focus, it is expected that reflected water waves from the breakwater can converge at the focus of the parabolic opening. Therefore, in certain conditions, the wave energy harvest can be multiplied if an oscillating buoy (OB)-WEC is placed at the focus position. Hereafter, the breakwater with parabolic openings is called 'parabolic breakwater' for convenience. Fig. 1a shows an example of such design. Actually, a few pioneer studies have already tested the efficiency improvement of wave energy harvest through a proper optimisation of the breakwater[5].

As a preliminary concept examination, a near-shore bottom-mounted breakwater is considered. The breakwater is assumed to be parallel with a straight coastline, so that incident waves can be considered to propagate perpendicularly towards the structure for convenience. The breakwater has an array of identical parabolic openings on its weather side. Each parabolic opening has its axis of symmetry parallel to the propagation direction of incident waves. An cylindrical OB-WEC with one degree of freedom (DoF) in the vertical direction (i.e. only with heave mode) is deployed on the axis of symmetry of each parabolic opening. Due to the geometric symmetry, the array model of OB-WECs in front of the breakwater can be equivalently considered as an individual OB-WEC in a wave flume. At the end of the flume is the breakwater unit with a parabolic opening. Figs. 1b and 1c show the top and side views of the physical model, respectively.

A right-handed Cartesian coordinate system $O - xyz$ is introduced in Fig. 1. The origin O is defined on the still free surface at the intersection of the flume's mid-surface and the tangential plane of breakwater's weather side. The x -axis points perpendicularly into the breakwater, and z -axis points vertically upward. The parabolic opening in the breakwater can be mathematically described by $y^2 = -2p(x - x_0)$. The focus and vertex of the parabola are at $\{x, y\} = \{x_f, 0\}$ and $\{x_0, 0\}$, respectively, with $x_f = x_0 - p/2$. The width of the parabolic opening is denoted

*Email: chongweizhang@dlut.edu.cn

†Email: dzning@dlut.edu.cn

‡Email: bteng@dlut.edu.cn

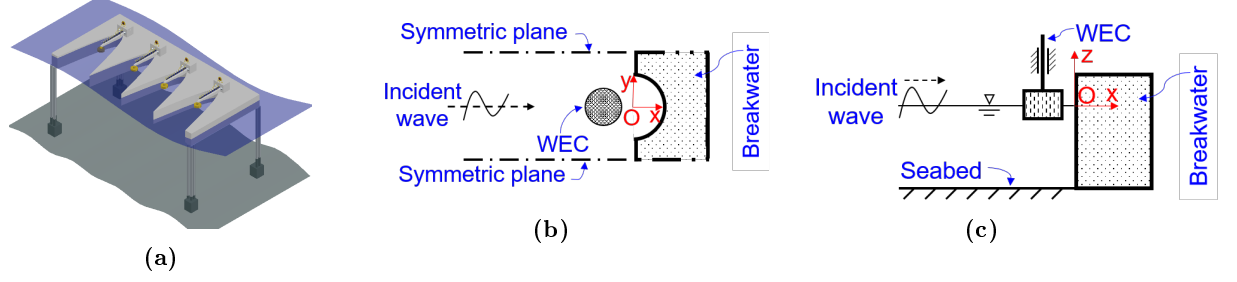


Fig. 1. Model of a parabolic OB-WEC breakwater: (c) design example; (b) top view; (c) side view

by B with shoulder points at $\{x, y\} = \{0, \pm B/2\}$. The distance between two shoulder points of neighbour openings is $2w$. The OB-WEC is rigid, whose heave motion is determined by Newton's Second Law as

$$M\ddot{s} + (B + B_{\text{PTO}})\dot{s} + Cs = F_{\text{FK}} + F_{\text{S}} \quad (1)$$

where M is the mass of the OB-WEC, B is the damping coefficient due to energy dissipation in the fluid, B_{PTO} is the damping coefficient associated with the Power-Take-Off system, C is the restoring coefficient, F_{FK} denotes Froude-Krylov (FK) force, F_{S} is the scattering wave force, and s , \dot{s} and \ddot{s} represent the vertical displacement, velocity and acceleration of the floating body, respectively. In this study, the case-dependent values of B and B_{PTO} are set to be zero to highlight the maximum motion response of an OB-WEC. Both F_{FK} and F_{S} are given using potential-flow theory. A linear numerical wave flume based on 3D boundary element method (BEM) is developed [6]. Wave field characteristics around this type of parabolic breakwaters and hydrodynamic properties of an OB-WEC installed on the breakwater will be investigated.

For the present model, the fluid domain is initially in stationary, when incident waves enter from the open boundary on the left hand side of the fluid domain. As the wave reaches the weather side surface of the breakwater, it is reflected back to the open boundary. The damping zone on the free surface near the open boundary is used to dissipate the waves propagating from the breakwater. In subsequent simulations, the length of the damping zone is set as 1.5 times the wave length L_d , i.e. $L_d = 1.5L_w$. The damping strength for the nondimensional numerical model is set as $\mu_0 = 1$.

The maximum wave height (MWH) distribution in the wave flume is first shown in Fig. 2. The MWH at a location in the wave flume is defined as the difference of the largest and lowest wave elevation appearing at that location for a specified time duration. In subsequent results, every MWH distribution map is normalized by the incident wave height H_0 , with the denotation H_w/H_0 . Fig. 2a shows the MWH distribution of reflected waves. The uniform MWH distribution of reflected waves indicates that the reflected waves have propagated through the whole wave flume and reached a steady state. Fig. 2b corresponds to the MWH distribution of the superposition of incident and reflected waves, which is called the 'full wave field' for convenience. It can be seen that peak values of the MWH distribution appear periodically along the x -axis. Two pentagrams at $x = 0.5L_w$ and L_w are marked in the figure. From their locations, it can be told that the peak values of the MWH for the full wave field can be found at a distance $0.5nL_w$ ($n = 1, 2, \dots$) away from the plane breakwater. Back to the wave energy application background, the OB-WECs are likely to be placed at a distance of $0.5L_w$ or L_w away from the breakwater when integrated into the plane breakwater.

Then, the wave field in front of a representative parabolic breakwater is illustrated. The following geometry parameters are chosen: $x_0 = 0.5$, $w = 0$, $p = 1$, and $B = 1$, with the focus position at $x_f = 0.5$. The wave length of incident waves are set as $L_w = 0.6$ and $L_w = 1.1$, respectively. Fig. 3 shows the MWH distribution of reflected waves. To guarantee a fully-developed wave field, the time duration of each simulation case is set as $2L/v_w$ with v_w as the phase velocity of incident waves. A hollow pentagram is marked in the wave field to indicate the

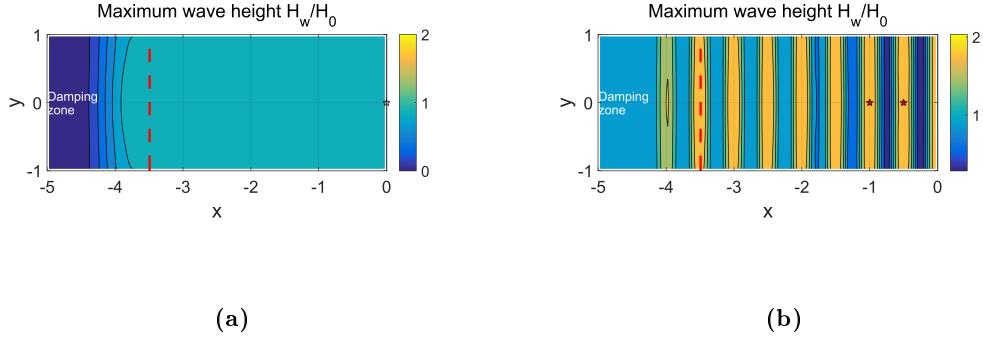


Fig. 2. Spatial distribution of the maximum wave height of (a) reflected wave field; (b) full wave field

focus position. From Fig. 3, it can be seen that the MWH of reflected waves have its peak value appearing at the focus position. In other words, reflected waves from the parabolic surface travel towards the focus, leading to a wave focusing at that position. Fig. 4 further gives the MWH

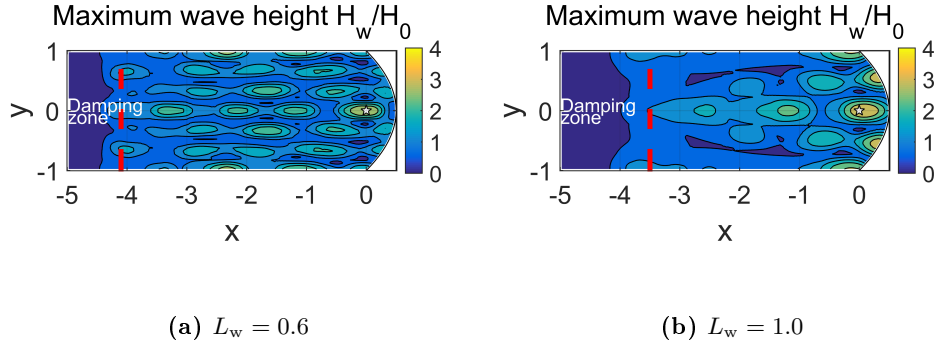


Fig. 3. Spatial distribution of the maximum wave height of reflected wave field, for (a) $L_w = 0.6$; (b) $L_w = 1.0$

distribution of the full wave field through a superposition of incident and reflected waves. Unlike the observation in Fig. 3, the peak MWH value for the full wave field does not always occur at the focus position. Two red pentagrams are marked in each sub-figure to indicate the position that is half and one wave length away from the vertex of the parabolic opening, respectively. It is found that the MWH at $x_{0.5L}$ and $x_{1.0L}$ can reach about four times the wave height of incident waves. For the case of $L_w = 1.0$, the peak MWH value can be found at $x_{0.5L}$, which is over four times the wave height of incident waves. Based on this fact, for a given wave environment with a dominant wave length L_w , the parabolic breakwater can be designed with its focus at $0.5L_w$ away from the vertex of the parabolic opening.

Further, an OB-WEC is placed at the target location. For simplicity, the OB-WEC is considered as a truncated circular cylinder only undergoing the heave motion. Fig. 5 compares heave histories of the floating buoy in front of the parabolic and plane breakwaters. It can be seen that after an instantaneous stage in the beginning the time history, the body motion tends to be steady gradually. At the near-steady state, the body motion amplitude is modulated, because the body motion consists of two oscillation components at the natural frequency of the body motion and the wave excitation frequency. Within the time duration between $t = 20T$ and $30T$, the oscillation amplitude of the body in front of the parabolic breakwater is about three times larger than that of the conventional plane breakwater. It is reasonable to attribute this motion amplification to the wave focusing effect of the parabolic breakwater. In practice, if the

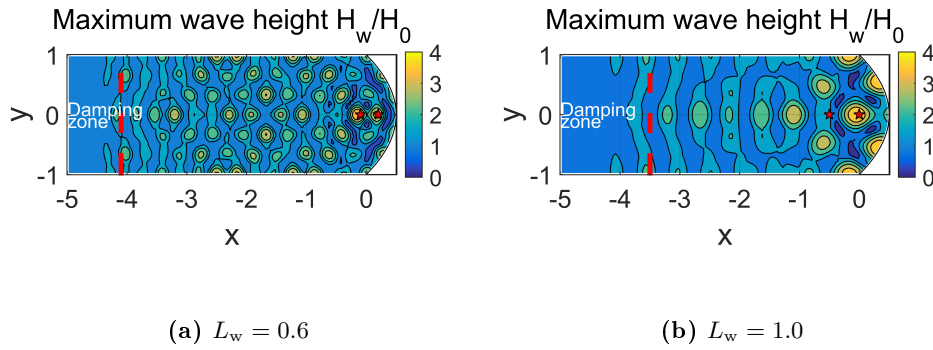


Fig. 4. Spatial distribution of the maximum wave height of full wave field, for (a) $L_w = 0.6$; (b) $L_w = 1.0$

geometry and size of the OB-WEC is optimized (for example, by adjusting the natural oscillation frequency of the OB-WEC to the dominant wave frequency), an even larger motion response can be expected. A more systematic hydrodynamic investigation of this WEC-breakwater model will be presented in the workshop.

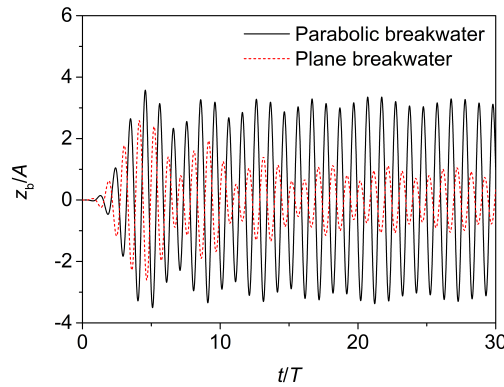


Fig. 5. Heave histories of an OB-WEC in front of parabolic and plane breakwaters

Acknowledgement: This study is supported by the National Science Foundation of China (Grant Nos. 51709038 and 51679036), Project funded by China Postdoctoral Science Foundation (No. 2018M630289), and the UK-China Industry Academia Partnership Programme (Grant No. UK-CIAPP \73).

References

- [1] J. Goggins and W. Finnegan, “Shape optimisation of floating wave energy converters for a specified wave energy spectrum,” *Renewable Energy*, vol. 71, pp. 208 – 220, 2014.
- [2] B. F. M. Child, *On the configuration of arrays of floating wave energy converters*. PhD thesis, Edinburgh, 2011.
- [3] M. E. McCormick, *Ocean Wave Energy Conversion*. New York: Dover Publications, 2007.
- [4] M. Mustapa, O. Yaakob, Y. M. Ahmed, C.-K. Rheem, K. Koh, and F. A. Adnan, “Wave energy device and breakwater integration: A review,” *Renewable and Sustainable Energy Reviews*, vol. 77, pp. 43 – 58, 2017.
- [5] H. Fernandez, G. Iglesias, R. Carballo, A. Castro, J. Fraguera, F. Taveira-Pinto, and M. Sanchez, “The new wave energy converter wavecat: Concept and laboratory tests,” *Marine Structures*, vol. 29, no. 1, pp. 58 – 70, 2012.
- [6] C. Zhang and W. Duan, “Numerical study on a hybrid water wave radiation condition by a 3d boundary element method,” *Wave Motion*, vol. 49, no. 5, pp. 525 – 543, 2012.